



On the use of bastnasite ore as a phosphor material



M. Mohapatra*, V. Natarajan, B. Rajeswari, A.R. Dhobale, S.V. Godbole

Radiochemistry Division, Bhabha Atomic Research Centre, Trombay, Mumbai 400085, India

ARTICLE INFO

Article history:

Received 28 March 2013

Received in revised form

10 June 2013

Accepted 16 July 2013

Available online 24 July 2013

Keywords:

Bastnasite
Luminescence
Rare earths
CIE indices

ABSTRACT

Bastnasite ore obtained from Indian Rare Earth (IRE) was investigated for its possible use as a phosphor material. The material was characterized by X-ray diffraction (XRD), energy dispersive X-ray fluorescence (EDXRF), photoacoustic spectroscopy (PAS), photoluminescence (PL) and electron paramagnetic resonance spectroscopy (EPR) techniques. XRD studies revealed the semi processed ore to be consisting of single phase CeO_2 with no other impurities. EDXRF studies revealed the presence of 'Th' and traces of 'Sm' along with 'Ce' in the sample. PAS studies revealed the presence of strong charge transfer from oxygen to cerium in the system. PL studies confirmed the presence of at least four trivalent rare earths, viz. Sm, Eu, Dy and Tb in the system in trace quantities. The emission spectrum and decay time data were evaluated. It was observed that the rare earth ions are situated at distorted sites in the system surrounded by defect centers. EPR studies confirmed the presence of Ce^{3+} in the system along with electron trapped in oxygen ion vacancies. CIE indices for the ore sample were evaluated and it was seen that the overall emission from the system was in the 'magenta' region of the visible spectrum. The emission intensities were also compared with that of commercial samples.

© 2013 Elsevier B.V. All rights reserved.

1. Introduction

In recent years, there is considerable interest in developing rare earth (RE) oxide powders for various applications in phosphor, catalysis and fuel cell industries [1–3]. Especially due to the higher chemical and thermal stability of the oxides as compared to the conventional sulfide based systems, these find enormous applications as phosphors in optoelectronic devices and flat panels displays.

Among the RE oxides, cerium oxide (ceria, CeO_2) is one of the most reactive one with a wide band gap of 5.5 eV and high dielectric constant ($\epsilon=26$) [4]. CeO_2 finds extensive use in phosphor industry as a host matrix for other RE and transition metal (TM) ion doping [5–7]. In addition, ceria is one of the most superior glass-polishing materials owing to its abrasive nature [8] and known to be used as a three-way catalyst in vehicle emission control systems [9]. Doped CeO_2 is used as an oxide-ion electrolyte in solid-oxide fuel cells (SOFC) [10]. It is also known to be added in silicon nitride and sintered zirconia as a minor additive to increase the toughness [11]. This also finds utility in solar cells, gates for metal-oxide semiconductor devices and sunscreen cosmetics [12].

One important aspect of this material is its remarkable similarity to PuO_2 in terms of physico-chemical and thermo-chemical properties. Therefore, this has been used as a surrogate for plutonium oxide [13].

Cerium being the most abundant metal among the rare earths, it is found in a number of mineral such as bastnasite, monazite, gadolinite, fergusonite, samarskite, xenotime, yttrocerite, cerite and allanite (also known as orthite), etc. Among these, bastnasite and monazite are the two most important sources of cerium [14].

Though one can find many literature reports on the electrical, luminescence and thermal properties of doped ceria, there is not much work on the characterization of ceria ores.

Through the present investigation, an attempt has been made to characterize a semi processed bastnasite ore of CeO_2 obtained from Indian mines.

2. Experimental

The bastnasite ore was obtained from Indian Rare Earths Limited, Mumbai, India. The crude bastnasite ore (LnCO_3F) was first calcined to remove volatile impurities after which it was leached with dilute HNO_3 . During this process, other rare earth ions get dissolved in the acid, while insoluble Ce (along with Th) gets precipitated [15]. In this manuscript, we refer to this dried precipitate as the semi processed ore. This semi processed ore was further characterized by X-ray diffraction (XRD), energy dispersive X-ray fluorescence spectroscopy (EDXRF), Photoacoustic spectrometry (PAS), photoluminescence (PL) spectroscopy and electron paramagnetic resonance spectroscopy (EPR).

XRD studies were carried out on a STOE X-ray diffractometer equipped with Ni filter, scintillation counter and graphite monochromator. The diffraction patterns were obtained using

* Corresponding author. Tel.: +91 22 25594093 ; fax: +91 22 25505151.

E-mail addresses: manojm@barc.gov.in, mohapatramanoj@gmail.com (M. Mohapatra).

monochromatic Cu-K α radiation ($\lambda=1.5406 \text{ \AA}$) keeping the scan rate at 1 s/step in the scattering angle range (2θ) of 10° – 70° . The K α_2 reflections were removed by a stripping procedure to obtain accurate lattice constants and grain.

EDXRF measurements were done on a Jordan Valley EX-3600M EDXRF spectrometer equipped with Rh source and Si(Li) detector.

For the PAS investigations, a home built PAS spectrometer was used [16]. The PAS unit consists of 250 W tungsten-halogen lamps, 0.25 M monochromator (model 82-410, Jarrell-Ash Ebert), PAS cell and lock-in amplifier (model – IE 1033, Unilock) designed and fabricated in-house.

PL data were recorded on an Edinburgh CD-920 unit equipped with Xe flash lamp with 10–100 Hz frequency as the excitation source. The data acquisition and analysis were done by F-900 software provided by Edinburgh Analytical Instruments, UK.

EPR experiments were performed on a Bruker ESP 300 spectrometer operated at X-Band frequency (9.60 GHz) equipped with 100 kHz field modulation. The 'g' values were calibrated relative to a 2,2 diphenyl-1 picryl hydrazil (DPPH) standard having $g=2.0036$. Samples were recorded both at room temperature (RT) and at liquid nitrogen temperature (LNT, 77 K). For this purpose, the Bruker temperature variation unit BVT 3000 was used.

3. Results and discussion

Ceria has a well known cubic fluorite structure. Fig. 1A shows the XRD patterns of the semi processed ore. The XRD pattern matched with that of CeO $_2$ in cubic fluorite structure with ICDD file no- 78-0694 (space group Fm3m (2 2 5)). The major reflections were from the crystallographic planes (1 1 1), (2 0 0), (2 2 0) and (3 1 1) [17]. Based on this data, the lattice parameters were evaluated to be $a=b=c=5.42 \text{ \AA}$ (± 0.01). For comparison, the standard ICDD pattern is also given in Fig. 1B.

Fig. 2 shows the raw EDXRF data for the sample in the energy range 1–20 keV. The spectrum is characterized by the presence of characteristic L-X-ray peaks due to Ce, Sm, Cu and Th. Thorium is expected to come in the sample during the precipitation, whereas samarium comes as an impurity in the ceria ore.

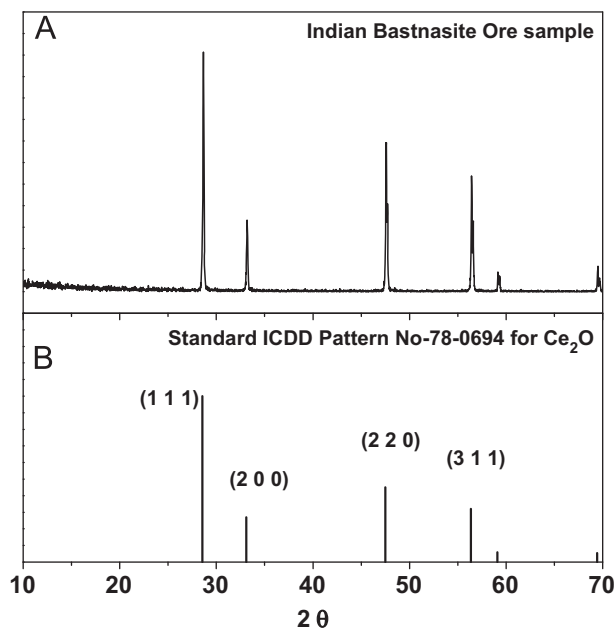


Fig. 1. (A) XRD patterns for the semi processed sample and (B) standard ICDD pattern for Ce $_2$ O $_3$ indicating the reflection planes.

The PAS spectrum for the semi processed ore sample is presented in Fig. 3. The spectrum is characterized by a broad peak at 364 nm corresponding to the Ce $^{4+}$ –O $^{2-}$ charge transfer band (CTB). No other absorption band could be seen in the sample.

The PL emission spectrum for the sample with 364 nm excitation is shown in Fig. 4. The spectrum is characterized by the presence multiple bands/peaks at 485, 564, 574, 592, 615, 675 and 725 nm.

To further confirm the assignments of the band positions to the respective rare earth ions, PL decay time measurements were carried out on the sample with 364 nm excitation and varying emission wavelength. The luminescence decay curves were recorded on 10 ms scale and fitted using the following exponential decay equation by an iterative process.

$$I(t) = A_i + \sum_{i=1}^n e^{-t/\tau_i}$$

here A_i is a scalar quantity, t, s are the times of measurement and τ_i are the decay time values (time taken for the excited state population to become $1/e$ of the starting value). The decay time

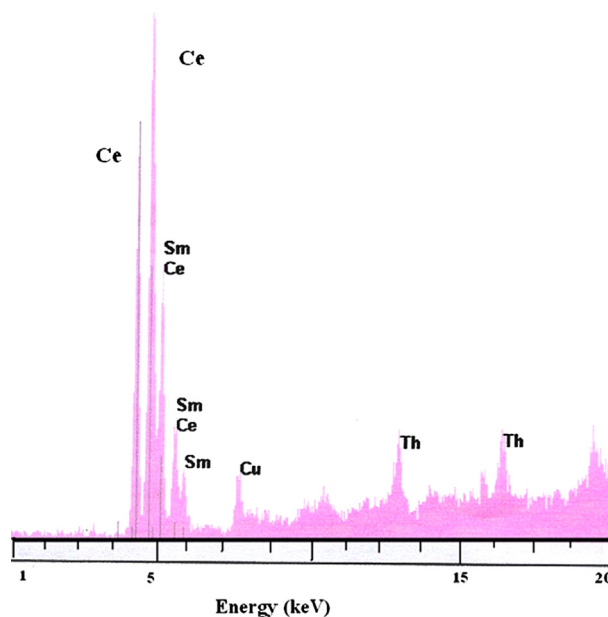


Fig. 2. EDXRF spectrum for the semi processed ore.

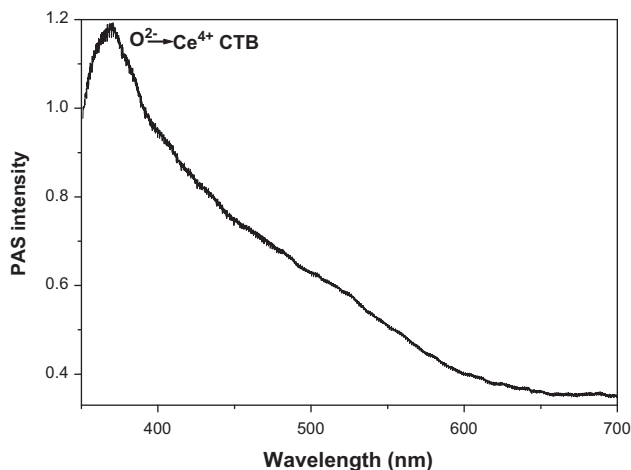


Fig. 3. PAS spectrum for the semi processed ore.

Download English Version:

<https://daneshyari.com/en/article/5400145>

Download Persian Version:

<https://daneshyari.com/article/5400145>

[Daneshyari.com](https://daneshyari.com)